Available online at www.sciencedirect.com
ScienceDirect
Acta Materialia 59 (2011) 2437–2446
Acta MATERIALIA
www.elsevier.com/locate/actamat

Fracture toughness and fatigue crack growth characteristics of nanotwinned copper

A. Singh [a,1], L. Tang [b,1], M. Dao [a,*], L. Lu [b,*], S. Suresh [a]

[a] Department of Materials Science and Engineering, Massachusetts Institute of Technology, Cambridge, MA 02139, USA
[b] Shenyang National Laboratory for Materials Science, Institute of Metal Research, Chinese Academy of Sciences, Shenyang 110016, China

Received 25 November 2010; received in revised form 20 December 2010; accepted 21 December 2010
Available online 1 February 2011

Abstract

Recent studies have shown that nanotwinned copper (NT Cu) exhibits a combination of high strength and moderate ductility. However, most engineering and structural applications would also require materials to have superior fracture toughness and prolonged subcritical fatigue crack growth life. The current study investigates the effect of twin density on the crack initiation toughness and stable fatigue crack propagation characteristics of NT Cu. Specifically, we examine the effects of tailored density of nanotwins, incorporated into a fixed grain size of ultrafine-grained (UFG) copper with an average grain size of 450 nm, on the onset and progression of subcritical fracture under quasi-static and cyclic loading at room temperature. We show here that processing-induced, initially coherent nanoscale twins in UFG copper lead to a noticeable improvement in damage tolerance under conditions of plane stress. This work strongly suggests that an increase in twin density, at a fixed grain size, is beneficial not only for desirable combinations of strength and ductility but also for enhancing damage tolerance characteristics such as fracture toughness, threshold stress intensity factor range for fatigue fracture and subcritical fatigue crack growth life. Possible mechanistic origins of these trends are discussed, along with issues and challenges in the study of damage tolerance in NT Cu.

Keywords: Nanotwins; Fracture toughness; Fatigue crack growth; Damage tolerance; Nanocrystalline copper

1. Introduction

Reducing the grain size of a material to enhance its strength has long been a strategy used in microstructure design [1–6]. In conventional microcrystalline metals and alloys (average grain dimensions typically bigger than 1 μm), grain refinement generally results in an increase in the resistance to fatigue crack initiation. In high cycle fatigue, this trend is reflected as a higher fatigue endurance limit (which is elevated with higher strength); the endurance limit is typically measured through cyclic-stress-controlled experiments on initially smooth laboratory specimens [7]. When the average grain size is refined to values typically below 100 nm, the resulting nanostructured metals exhibit significantly elevated strength and strain rate sensitivity and much lower activation volume, as well as improved resistance to corrosion, fatigue crack initiation for long life as seen in the fatigue endurance limit, and monotonic and cyclic wear [8–13] in comparison to microcrystalline metals and alloys [3,5,6]. However, such beneficial effects of grain size reduction are also commonly accompanied by reductions in ductility. The drop in ductility is ascribed to significant constraints encountered in accommodating plastic strain through the generation and accumulation of dislocations in the nanograined (NG) metals [3,5,6,14]. Furthermore, grain refinement into the nanocrystalline regime is known to degrade different metrics of damage tolerance including fracture toughness and the resistance to stable subcritical crack growth under monotonic and cyclic loading, especially at lower values of stress intensity factor range (the so-called near-threshold regime with crack growth rates typically smaller than 10^{-6}

* Corresponding authors.
E-mail addresses: llu@imr.ac.cn (L. Lu), mingdao@mit.edu (M. Dao).
[1] These authors contributed equally.

1359-6454/$36.00 © 2011 Acta Materialia Inc. Published by Elsevier Ltd. All rights reserved.
doi:10.1016/j.actamat.2010.12.043

mm cycle^{-1}) where most of the fatigue fracture life is expended [7,8,10,15].

In addition to these effects on mechanical properties, grain refinement, especially in the nanocrystalline regime, is also known to have a deleterious effect on electrical conductivity [16–19] and resistance to electromigration [20].

To date, there is limited information available on the fatigue properties of ultrafine-grained (UFG) and nanograined (NG) materials. Earlier studies included high cycle fatigue experiments performed on nanocrystalline Cu produced by inert gas condensation [21] in order to ascertain the stability of microstructure under cyclic loading. These experiments documented 30% increase in grain size due to repeated, cyclic loading along with the surface being populated with parallel "extrusions" seemingly similar to persistent slip bands (PSBs) observed in coarse-grained (CG) Cu and single crystals [7]. Strain-controlled fatigue tests [22] comparing UFG Cu prepared by severe plastic deformation (SPD) and CG Cu showed that the latter has a longer total fatigue life than the former, and that the surface of the fatigued UFG specimen showed extrusions similar to those found in NG Cu [21]. In addition, cyclic softening was observed in Cu prepared by SPD [23]. However, it has been found [24] that annealing treatment improves the low cycle fatigue life in strain controlled cyclic tests on UFG materials produced by equal channel angular pressing (ECAP). Cyclic softening in UFG Cu produced by ECAP was also ascribed to dynamic recrystallization and subsequent grain growth which was observed after strain controlled cyclic loading on Cu specimens produced by ECAP [25]. Unlike UFG metals prepared from SPD techniques, electrodeposited NG Ni with an average grain size of 40 nm displayed cyclic strain hardening under tension–tension cyclic loading. The deformation was also found to be dependent on the frequency of applied loading [26]. Stress-controlled cyclic loading applied on bulk Ni–18 wt.%Fe alloy with an average grain size of 23 nm and produced by pulsed electrodeposition exhibited an endurance limit of just 13% of the yield stress, which was surprisingly low compared to the trend shown by other metals [27]. Fracture and fatigue studies [28] done on the same bulk Ni–18 wt.%Fe alloy with an average grain size of 23 nm demonstrated limited values of fracture toughness owing to nanovoid coalescence at the grain boundaries. In the near-threshold regime of stable fatigue crack growth, the crack path was found to be non-tortuous as seen through scanning electron microscopy (SEM). Focused ion beam confirmed the results obtained earlier from atomistic simulations [29] that the microcracks are initiated close to the primary crack by the process of nanovoid coalescence. Xie et al. [30] performed experiments on electrodeposited Ni sheets (average grain size 26 nm) and CG Ni in order to determine the difference in the modes of fatigue crack nucleation. It was found [30] that for CG Ni crack nucleation occurred in a diffused manner in that a population of cracks was observed whereas for NG Ni there was one principal crack and dislocation cell structures with an average size of 108 nm were observed along the main crack.

Mirshams et al. [15] found that the fracture toughness of pure NG Ni produced by pulsed electrodeposition decreased with an increase in annealing temperature. Their results were rationalized using the "cluster model" [31]. Here the claim is that a large number of nonequilibrium vacancies formed during the process of recrystallization of nanocrystalline materials would segregate and condense into clusters preferentially residing at the grain boundaries. These clustered vacancies would weaken the material, and the number and size of these clusters would increase with an increase in annealing temperature.

Opposite trends, however, were observed for carbon-doped NG Ni in that the fracture toughness increased with an increase in annealing temperature. Charpy impact energy tests on electrodeposited Co showed that the toughness decreases as the grain size is refined close to 18 nm [32]. This trend has also been corroborated by fracture studies on α-Fe and Al [33], which have shown that fracture toughness decreases with grain refinement. Stress-controlled cyclic loading experiments conducted on electrodeposited Ni showed an improvement in fatigue life and endurance limit with grain refinement in the <100 nm regime. However, stable crack propagation experiments on CG, UFG and NG Ni revealed diminishing fatigue crack growth threshold values with grain refinement [8,10].

The foregoing discussion of prior work clearly illustrates that: (i) there has been very little systematic work on the fracture and fatigue crack growth characteristics of nanograined metals and alloys; (ii) the limited experimental information available to date generally appears to indicate a significant reduction in damage tolerance with grain refinement into the nanocrystalline regime; and (iii) the loss of resistance to fatigue crack growth with grain refinement in NG metals, especially in the near-threshold regime, mirrors the trend observed in their CG counterparts [8,10].

Significant strengthening due to grain refinement arises from the obstruction of dislocation motion at nanoscale grain boundaries. Similar strengthening can also be achieved through the introduction of initially coherent twin boundaries within UFG metals. Recent studies [34–38] have shown that when a polycrystalline ensemble of UFG copper (with average grain size in the range of 100–1000 nm) is populated with initially coherent, mechanically and thermally stable nanoscale twins (where the twin width or spacing is on the order of tens of nanometers), the ensuing structure exhibits deformation characteristics that mirror those of nanograined copper whose average grain size is comparable to the twin spacing in the nanotwinned (NT) copper. In other words, when nanotwins are introduced in the UFG metal during pulsed electrodeposition, the material exhibits strengthening characteristics and strain rate sensitivity comparable to those of a nanograined metal without twins [34,35,38]. The coherent NT boundaries act as barriers to dislocation motion just as grain boundaries do [36,37,39]. The pile-up of dislocations at

an incoherent GB leads to a stress concentration that can result in the nucleation of new dislocations on the other side of the boundary without altering the character and energy of the GB. Since the structure of the GB is not altered, dislocations usually do not glide along the boundary. This limited capability of GBs to accommodate dislocations during deformation manifests in reduced ductility despite promoting increased strength. On the other hand, the twin boundaries are not only capable of accommodating dislocations, but also facilitate glide of dislocations along the boundary, given their significant local plastic anisotropy [6,35].

Post-deformation studies of NT specimens have shown high dislocation density in the vicinity of the twin boundaries [35,40]. These attributes of NT copper appear to facilitate not only a potent mechanism of strengthening through the control of twin density at the nanoscale without any change in grain size, but also help retain a significant fraction of ductility when strengthening is achieved through NT refinement. As a result, nanotwinned metals offer the potential for engineering mechanical properties with optimized combinations of strength and ductility for a variety of structural applications by circumventing issues related to the severe loss of ductility, which are serious drawbacks of grain refinement strategies involving nanograined materials [5,6]. The fact that the electrical resistivity of coherent twin boundaries is one order of magnitude lower than high-angle grain boundaries also enhances its range of applications [41,42].

Only a few cyclic loading studies have been carried out so far on NT materials, and these have demonstrated enhanced mechanical stability of twin boundaries. For example, multilayer copper/copper specimens with nanoscale twins produced by magnetron sputtering have been shown to exhibit considerable microstructural stability and hardness retention even under fatigue loading and indentation [43]. The twin lamellae thickness dependence of fatigue endurance limit of the nanotwinned Cu (NT Cu) was also studied by conducting cyclic tension–tension tests under constant stress amplitude at room temperature [44]. Initial results suggest that both the high cycle fatigue life and fatigue endurance limit increase with a decrease in the twin lamellae thickness [44]. Cyclic studies done on NG Ni–Fe alloy with growth twins have shown considerable grain growth and detwinning in the path of the fatigue cracks, with little microstructural change observed in grains removed from the crack [45]. In addition, large-scale atomistic simulations to model the damage tolerance behavior of NG materials (average grain size ~20 nm) with nanoscale twins have suggested the possibility of an improvement in fracture toughness with an increase in twin density [46,47].

Copper produced by dynamic plastic deformation (DPD) under conditions of high strain rate and cryogenic temperatures has a microstructure with a mixture of deformation twins and nanograins. Qin et al. [48] have shown that increasing the strain while preparing the specimen leads to an increase in fracture toughness on account of increase in the concentration of deformation twins in the structure. However, the highly heterogeneous microstructure of DPD Cu comprises both deformation twins and nanograins, and the percentage of both of them increases with the imposed strain, so it is difficult to elucidate the isolated role of twin boundaries in influencing the fracture toughness. To our knowledge, no experimental studies of the key damage tolerance characteristics involving systematic fracture toughness measurements and fatigue crack growth behavior of nanotwinned metals and alloys have been reported to date.

The use of pulsed electrodeposition (PED) to produce nanotwinned copper, while enabling the manipulation of the grain size and twin density by controlling such parameters as current density and time, has thus far resulted in producing fully dense NT specimens in the form of thin foils only. As a result, it is presently not feasible to perform "valid", plane strain fracture toughness or subcritical plane strain crack growth studies of fully dense, pure nanotwinned copper produced by PED. Despite this limitation, careful experiments could be designed to critically assess the structural effects of introducing nanotwins in UFG Cu on the relative intrinsic resistance to fracture toughness, fatigue crack growth and damage tolerance by performing linear elastic fracture experiments under plane stress conditions.

With the aforementioned background information, this paper reports the outcome of systematic experiments on the effects of controlled variations in nanotwin density in a UFG copper with a fixed grain size of approximately 450 nm. The present investigation therefore allows the effects of varying yield strength through the control of nanotwin density on fracture resistance and fatigue crack growth response to be isolated from any effects of grain size. Tensile tests were conducted on three specimens with different twin densities but with the same grain size, and their strength and ductility were determined. Damage tolerance was studied by introducing a crack of known length and applying displacement-controlled loading to the specimen until the onset of stable fracture. Subsequently, the stable crack propagation response was studied in precracked specimens by optically monitoring the length of the crack until catastrophic failure. Possible mechanistic origins of the observations are postulated and comparisons are made between the relative roles of grain and twin boundaries in influencing subcritical fatigue crack growth characteristics and fracture toughness under plane stress conditions.

2. Materials and methods

2.1. Materials

PED was used to synthesize high-purity copper specimens with nanoscale growth twin lamellae from an electrolyte of $CuSO_4$. The grains were equiaxed and the average grain size for all the specimens was 400–500 nm, but the

twin density was varied by modifying the electrodeposition parameters. Two specimens, one with the highest concentration of twin boundaries with an average twin lamellar spacing of 32 ± 7 nm (hereafter referred to as HDNT Cu, i.e. high density nanotwinned Cu) and the other with a relatively low density of twins with an average twin lamellar spacing of 85 ± 15 nm (LDNT Cu: low density nanotwinned Cu), were produced. The third control specimen, UFG Cu with essentially the same grain size but with no significant concentration of twins, was prepared by direct-current PED. The density of the as-deposited specimens was measured to be 8.93 ± 0.03 g cm^{-3}. The purity of the as-deposited copper was found to be more than 99.998 at.%, with less than 8 ppm S content. Chemical analysis also showed hydrogen and oxygen levels to be less than 15 and 20 ppm, respectively. The specimen preparation procedure and the structural characterization of the NT Cu are discussed in detail elsewhere [41].

2.2. Experimental methods

Three different kinds of mechanical experiments were performed in order to determine mechanical properties involving smooth tensile specimens, fracture toughness tests and stable fatigue crack propagation experiments. Details of these experimental methods and data analysis are described below.

2.2.1. Tensile tests

The tensile test specimens were made of a dog-bone shape, with a length of 16 mm, that was prepared using an electrodischarge machine (Fig. 1a). The thickness of all the smooth specimens is approximately 40 μm and the gauge length is 4 mm. Quasi-static tensile tests were conducted on all the specimens at room temperature on a Tytron 250 (MTS Systems Corporation, Eden Prairie, MN, USA) microforce testing system (MTS) at a strain rate of 6×10^{-3} s^{-1}. These tests yielded basic mechanical properties such as yield strength, tensile strength, strain to failure and ductility. The specimen strain was measured by a MTS LX300 laser extensometer.

2.2.2. Fracture toughness determination

Two specimens of each condition (HDNT, LDNT and UFG Cu) with similar dimensions were tested (Fig. 1b). A fatigue precrack was initiated to a depth of 1.5 mm in all the specimens. The specimens were gripped all along their width, as shown in Fig. 1c. Subsequently, monotonic loading was applied under displacement control mode at a rate of 0.5 mm min^{-1} on the Tytron 250 MTS. The displacement was allowed to increase until the crack propagated catastrophically to fracture. The displacement, δ, was plotted as a function of load, P, and a tangent line was drawn to the linear part of the initial P vs. δ curve. Subsequently a line having a slope of 95% of the tangent line was drawn. The point at which the 95% line intersected the load–displacement curve was the taken as the load, P_Q,

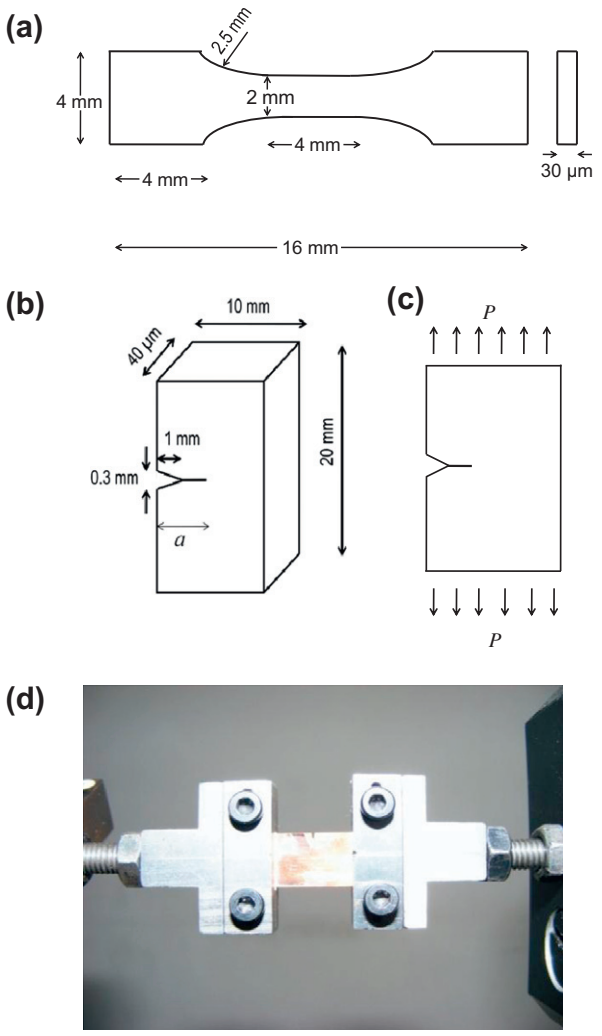

Fig. 1. (a) Schematic of the dog-bone-shaped specimen used for tensile testing. (b) Specimen geometry for fracture toughness test and stable fatigue crack propagation experiment. (c) Loading configuration for applying monotonic load to determine fracture toughness using the P–δ method. (d) Experimental set-up for studying the fatigue crack propagation, where the specimen was subject to tension–tension cyclic loading, with the ratio of the minimum load (stress intensity factor) to the maximum load (stress intensity factor), $R = 0.1$.

at which unstable crack growth ensued. This load was used to determine the fracture toughness estimates for the different materials studied, as described below. Further details of this method can be found in [49].

The mode I stress intensity factor (K_I) directly ahead of a sharp crack can be expressed in terms of the nominal stress applied on the specimen (σ), crack length (a), the specimen width (w) and the shape factor $f(\frac{a}{w})$ [7]:

$$K_I = \sigma\sqrt{a} f\left(\frac{a}{w}\right) \tag{1}$$

The shape factor $f(\frac{a}{w})$ depends on the geometry of the specimen and the loading conditions [7]. Fixed-end displacement loading was used in the present study for both fracture toughness estimation using the P–δ curve and subcritical crack growth measurement rather than pin-loading

(which can induce bending and wave form degradation); rigid grips help ensure uniform waveforms especially at frequencies above 5 Hz. A model based on the finite element (FEM) that employs the commercial software package ABAQUS (SIMULIA, Providence, RI, USA) was constructed for the geometry shown in Fig. 1c and computations were performed with the final aim of estimating $f(\frac{a}{w})$ in terms of $(\frac{a}{w})$ for the present loading configuration and geometry. The J integral for $(\frac{a}{w})$ values ranging from 0.1 to 0.7 was obtained through the simulations. The value of $f(\frac{a}{w})$ in turn was extracted from J from Eq. (2) for plane stress [7]:

$$f\left(\frac{a}{w}\right) = \sqrt{\frac{JE}{a\sigma^2}} \tag{2}$$

Using the above analysis, the shape factor was found as given in Eq. (3), and it is used to evaluate the stress intensity factor in all the cases:

$$f\left(\frac{a}{w}\right) = 1.94 + 0.81\left(\frac{a}{w}\right) - 2.40\left(\frac{a}{w}\right)^2 + 4.42\left(\frac{a}{w}\right)^3 \tag{3}$$

Fracture toughness is obtained by using Eq. (4), where B is the specimen thickness, w is the width of the specimen and a is the crack length at which the crack begins to propagate catastrophically:

$$K_C = \frac{P_Q}{BW}\sqrt{a} f\left(\frac{a}{w}\right) \tag{4}$$

However, in order to evaluate K_C for the imposed loading conditions using Eq. (4), it is necessary to ensure that the small-scale yielding (SSY) condition of linear elastic fracture mechanics (LEFM) analysis holds. This condition requires that the size of the plastically deformed material ahead of the crack tip should be small compared to all characteristic dimensions, including the length of the crack and the size of the uncracked ligament. The values of plastic zone radius, r_p, under conditions of plane strain and plane stress are given, respectively, by [50]

$$r_p = \frac{1}{6\pi}\left(\frac{K_I}{\sigma_y}\right)^2 \text{(plane strain)} \tag{5}$$

$$r_p = \frac{1}{2\pi}\left(\frac{K_I}{\sigma_y}\right)^2 \text{(plane stress)} \tag{6}$$

where σ_y is the material yield strength. According to the ASTM Standard E399 [51] $(a, w-a, B) \geqslant 25r_p$ for a valid plane strain fracture toughness test. Evaluating $25r_p$ using Eq. (5) and comparing it to the thickness B of the specimens lead to the inference that $B << 25r_p$ for the present specimens. Therefore all the specimens tested in this work are more representative of plane stress conditions than plane strain. Thus Eq. (6) is used to determine r_p for all the cases to assess the validity of the data points. As discussed earlier, high-quality NT Cu specimens can only be made at this time in relatively thin foils less than a few hundred micrometers in thickness. Consequently, the fracture toughness values reported here should be taken to represent broad material trends that arise due to controlled micro- and nanostructural variations, and relative values of damage tolerance characteristics of the different material conditions studied, not as true indicators in intrinsic, geometry-independent material fracture resistance.

2.2.3. Stable crack propagation experiments

Fatigue crack growth experiments were performed on two specimens of each condition (HDNT, LDNT and UFG Cu) at room temperature (approximately 25 °C and 50% relative humidity). The specimen dimensions are indicated in Fig. 1b. An initial cut was made using a sharp blade ahead of the notch tip before subjecting the specimen to fatigue in tension–tension cyclic loading in order to facilitate the formation of a precrack. The specimens were subsequently electropolished to relieve any surface residual stresses that could possibly arise from the introduction of the notch and specimen preparation. Subsequently an initial mode I fatigue precrack was introduced at the notch tip to a distance of 0.36 mm ahead of the notch tip (tip radius ~250 μm) by applying tension–tension cyclic loading at a load ratio of 0.1 and frequency of 10 Hz through a servohydraulic machine. Data gathered during this initial fatigue precracking process were not included in subsequent fatigue crack growth rate analysis in order to avoid possible effects of initial notch-tip region on the inferred fatigue fracture characteristics. The specimen was gripped along its entire width, as can be seen in Fig. 1d, and the experiment was performed under load-controlled conditions. The crack length was monitored through an optical microscope, and the crack length a was continuously tracked as a function of the number of fatigue cycles N. The value of K_I was determined from Eq. (1) using the value of $f(\frac{a}{w})$ given by Eq. (3). The fatigue crack growth rates and fracture toughness for all the specimens were estimated from a plot of $\log_{10}(da/dN)$ vs. $\log_{10}\Delta K$.

Microstructural characterization on the surface of fatigued samples was performed in a scanning electron microscope (Nova Nano-SEM 430) at a voltage of 18 kV.

3. Results

3.1. Tensile properties

The tensile properties of all the specimens were measured at room temperature, and are listed in Table 1. It is seen that increasing twin density leads to high values of strength without compromising ductility. This is consistent with the previous work done to investigate the effect of twin density on the tensile properties of NT Cu.

It can be seen that HDNT Cu shows the highest value of yield strength and tensile strength without a significant loss of ductility. The values of fracture toughness obtained from the P–δ curve and from the da/dN vs. ΔK curve indicate that increasing twin density leads to increased fracture toughness values.

Table 1
Values of yield strength, tensile strength, ductility and fracture toughness for HDNT, LDNT and UFG specimens.

Specimen	$\sigma_{0.2}$ (MPa)	σ_{ts} (MPa)	ε_{ts} (%)	K_{IC} (MPa$\sqrt{m}$) from the P–δ method	K_{IC} (MPa$\sqrt{m}$) from the da/dN vs. ΔK curve
UFG Cu	340 ± 30	430	12	12.9	14.9
LDNT Cu	500 ± 50	530	2.7	14.8	17.5
HDNT Cu	720 ± 50	820	5.6	17.2	22.3

3.2. Fracture toughness estimation from the P–δ curve

Fig. 2 shows a plot of engineering stress vs. displacement for all the specimens. To normalize the force variations due to sample thickness variations, nominal engineering stress (P/Bw) is used instead of the loading force P. Table 1 shows the values of the fracture toughness obtained from the P–δ curves, illustrating that decreasing twin lamellae spacing leads to enhanced fracture toughness.

3.3. Stable fatigue crack propagation

Fig. 3 shows a plot of the change in crack length vs. the number of cycles when multiple load-controlled cycles with an initial ΔK of 6 MPa$\sqrt{m}$ are imposed on the specimens. This leads to the inference that a decrease in twin lamellar spacing leads to smaller crack length change over the full range of cycles. In addition, the rate of increase in crack length with respect to the number of cycles is also smaller in the case of HDNT specimen, as can be seen from the slope of the curves at any point. Thus increasing the twin density appears to lead to an improvement in fatigue life under stable crack propagation.

Using a less stringent condition than prescribed in ASTM E399 [51] for the validity of SSY, i.e. $(a, w-a) > 15r_p$, Fig. 4a shows the variation of fatigue crack growth rate $\log_{10}(\mathrm{d}a/\mathrm{d}N)$ vs. $\log_{10}\Delta K$. If we define the fatigue transition threshold ΔK_T as the value of stress intensity factor range at which the crack growth transitions from

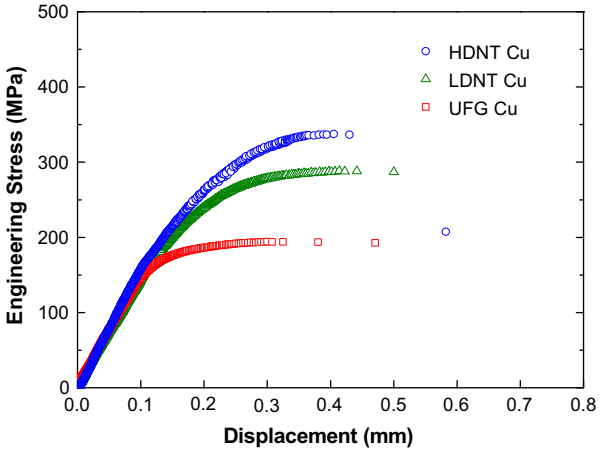

Fig. 2. Engineering stress vs. displacement plot of HDNT, LDNT and UFG specimens which were precracked to 1.5 mm prior to the fracture experiment.

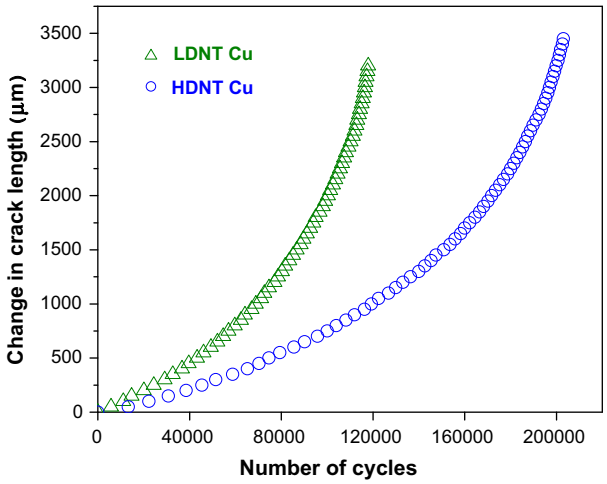

Fig. 3. A plot of the change in crack length vs. the number of cycles with an initial ΔK of 6 MPa$\sqrt{m}$ for the HDNT and LDNT specimens, demonstrating that increasing twin density leads to a decreased rate of fatigue crack growth.

stage I (near threshold mechanisms of crack growth) to stage II (Paris regime [7]) of subcritical crack growth, then it can be seen from the plot that the fatigue transition threshold is increased with an increase in twin density. The high twin density specimen also displays the smallest crack growth rate at any value of ΔK. Thus introduction of nanoscale twins appears to impart improved fatigue crack growth life in UFG Cu. This behavior of nanotwinned metals is in distinct contrast to prior results on nanograined metals that show a higher endurance limit but poorer resistance to fatigue crack growth upon grain refinement [8,10]. However, in our experiments HDNT Cu shows higher yield strength and thus greater crack initiation resistance, as well as a longer stable crack growth life. Fig. 4b shows that some of the data points become invalid if the stricter validity condition for SSY required in the ASTM E399 standard is imposed for the use of K in characterizing fatigue crack growth, which is $(a, w-a) > 25r_p$ from Eq. (5). However, even after imposing this stricter condition, the data obtained for both the specimens of HDNT Cu remain valid and for LDNT Cu data one specimen out of two continues to be valid. For UFG Cu, the data turn out to be invalid. However, since UFG Cu has the lowest yield strength, and hence the largest plastic zone size at any given K, of the three conditions employed in this study, any effect of plasticity would be expected to be more "forgiving" for fatigue fracture in that UFG Cu would be expected to result in slower crack growth rates if violation

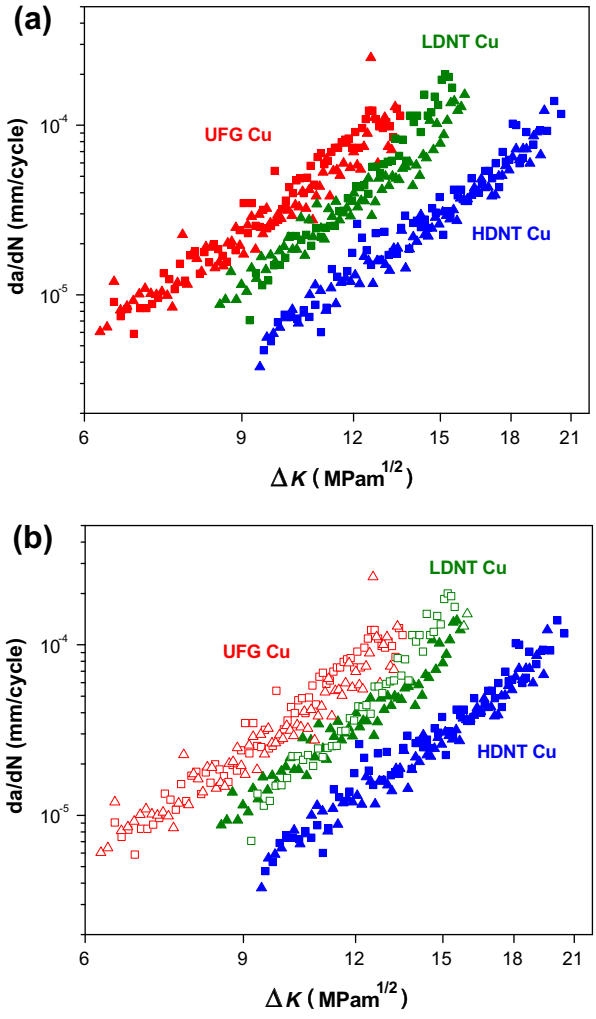

Fig. 4. (a) Variation of da/dN vs. $\log_{10}\Delta K$, showing that increasing twin density leads to the highest value of fatigue transition threshold ΔK_T and lowest crack growth rates for all values of ΔK. The validity condition for small-scale yielding (SSY) is taken to be $(a,\ w-a) \geqslant 15r_p$ for use of LEFM to characterize crack growth using ΔK. (b) Illustration on how some data points in (a) become invalid (marked by open symbols in (b)) if the SSY condition is made stricter to require that $(a,\ w-a) \geqslant 25r_p$.

of SSY were to alter the trends. With such an expectation, it is evident, even with the stricter specimen size requirement for valid use of stress intensity factor in Fig. 4b, that increasing twin density leads to an increase in resistance to fatigue crack growth.

Fracture toughness can also be estimated using the value of K_{max} at which fatigue crack growth rapidly transitions from subcritical to catastrophic failure. Specifically, this transition is taken as the maximum stress intensity factor corresponding to the ΔK at which there is a rapid rise in the slope of the $\log_{10}(da/dN)$ vs. $\log_{10}\Delta K$ curve immediately preceding catastrophic fracture in Fig. 4a. (Note that $K_{max} = \Delta K/(1-R)$.) Table 1 lists the relative fracture toughness estimates so obtained for the three materials studied in this work. The fracture toughness estimated in this way also shows the highest crack initiation toughness for the largest density of nanotwins, fully consistent with the estimates obtained from the P–δ curves in the quasi-static fracture toughness tests described earlier. Thus increasing the twin density in UFG Cu appears to render it more defect-tolerant.

4. Discussion

Many studies on conventional microcrystalline materials have shown that decreasing the grain size leads to a lower value of fatigue crack growth threshold ΔK_{th}, lower fatigue crack growth transition threshold ΔK_T and higher nominal driving force for fatigue crack growth close to the threshold regime [7,8]. In the present study the grain size was kept constant for all specimens, but another structural length scale, i.e. the nanotwin lamellar spacing, was varied. The impediment to dislocation motion due to the presence of twin boundaries is seen to result in higher strength, but the nanotwins also lead to higher values of ΔK_T (Fig. 5), lower crack growth rate and higher fracture toughness.

It is well known from studies of microcrystalline materials that fatigue crack growth rates close to the threshold regime are very sensitive to the microstructure, loading ratio and environment [7]. During stable near-threshold fatigue crack growth in microcrystalline metals and alloys, the plastic zone size is typically smaller than the grain size and crack growth occurs predominantly by planar slip in the direction of the primary slip system (so-called stage I crack growth). Since such crack growth occurs by single shear, the crack can continue to propagate locally along the primary slip plane within the grain, away from the nominal mode I growth plane, until deflected by an obstacle such as a high-angle grain boundary. As can be seen in Ref. [10], a larger grain size leads to higher tortuosity as the crack continues along a non-mode I deflected path. Higher

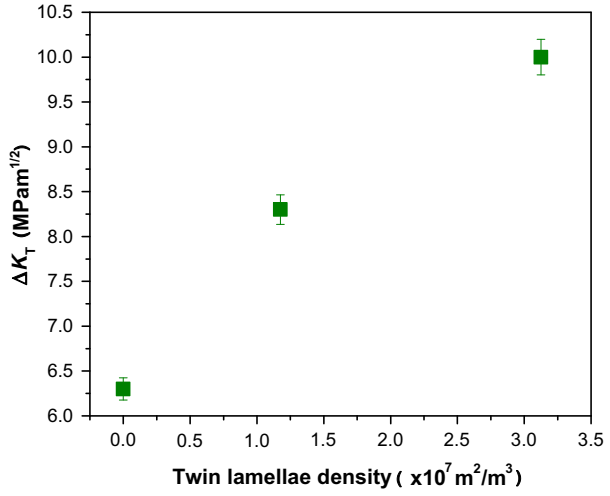

Fig. 5. Variation of the fatigue crack growth transition threshold (ΔK_T) as a function of twin density. Increasing twin density is beneficial for damage tolerance as ΔK_T is increased with a decrease in twin lamellar spacing.

tortuosity in crack growth leads to a smaller driving force for crack advance and a smaller effective crack growth rate [7,52]. Besides, larger grain size can promote bigger surface asperities, which also contribute to enhanced crack closure; this results in reduced crack growth rates at a given nominal value of stress intensity factor range [7,52].

In the present study the grain size was kept constant in all the materials but the twin density was varied. The fact that increasing the twin density leads to an improvement in fatigue crack growth life may be better understood in terms of the following arguments. First, grain boundaries and twin boundaries influence subcritical fatigue crack growth in stage I in different ways due to the strong dependence of crack propagation on crystallography. The twin boundaries inside each grain are parallel to one another and for face-centered cubic (fcc) metals the twin boundaries are also the (1 1 1) slip planes. Due to the strong plasticity anisotropy, shear deformation parallel to the twin boundaries is much easier than that in slip systems that have slip planes not parallel to the twin planes [6,35]. This crystallographic preference to move along a single slip plane would not be seen in UFG Cu without twins in which the crack can move along all slip systems (where the direction within each grain along the crack path would be determined by the local driving force). In nanotwinned Cu, a stage I fatigue crack would likely be parallel to the twinning planes within a grain, since twin boundaries unlike grain boundaries cannot veer the propagating crack back to the direction perpendicular to the loading direction (until the crack hit the next grain with a different twin boundary orientation). Thus the crack path tortuosity, size of the crack surface asperities and mismatch between the crack faces would be mainly influenced by the grain size but not the twin lamellae spacing. SEM images of the crack profiles also reveal this, as can be seen in Fig. 6, where the crack profiles of all the specimens bear close resemblance to each other in terms of crack path tortuosity, surface roughness and deflection angle on account of having similar grain sizes. Secondly, the fact that decreasing twin lamellar spacing improves fatigue life implies that strength alone as a parameter could be beneficial for stable crack growth life if other parameters are kept fixed for the present materials. Indeed, higher yield strength leads to a lower value of the maximum crack tip opening displacement. The value of the maximum or instantaneous crack tip opening displacement (CTOD) at $K = 6\ \mathrm{MPa}\sqrt{\mathrm{m}}$ for the three specimens can be estimated using the formula:

$$\mathrm{CTOD} = d_n \frac{K_I^2}{E\sigma_y} \tag{7}$$

The value of d_n varies from 0.3 to 0.8 as n changes from 3 to 13 [53]. The CTOD values for the HDNT, LDNT and UFG specimens are estimated to be 250, 360 and 528 nm respectively when d_n is taken as 0.6. The previous discussion showed that the height of the microstructural surface asperities depends on the grain size and not on the twin density, and hence it can be deduced that a higher twin density would induce relatively more roughness-induced crack closure due to a smaller value of CTOD, leading to better stable crack growth life under cyclic loading. Some earlier studies that formulated empirical models to ascertain the fatigue crack growth threshold and fatigue transi-

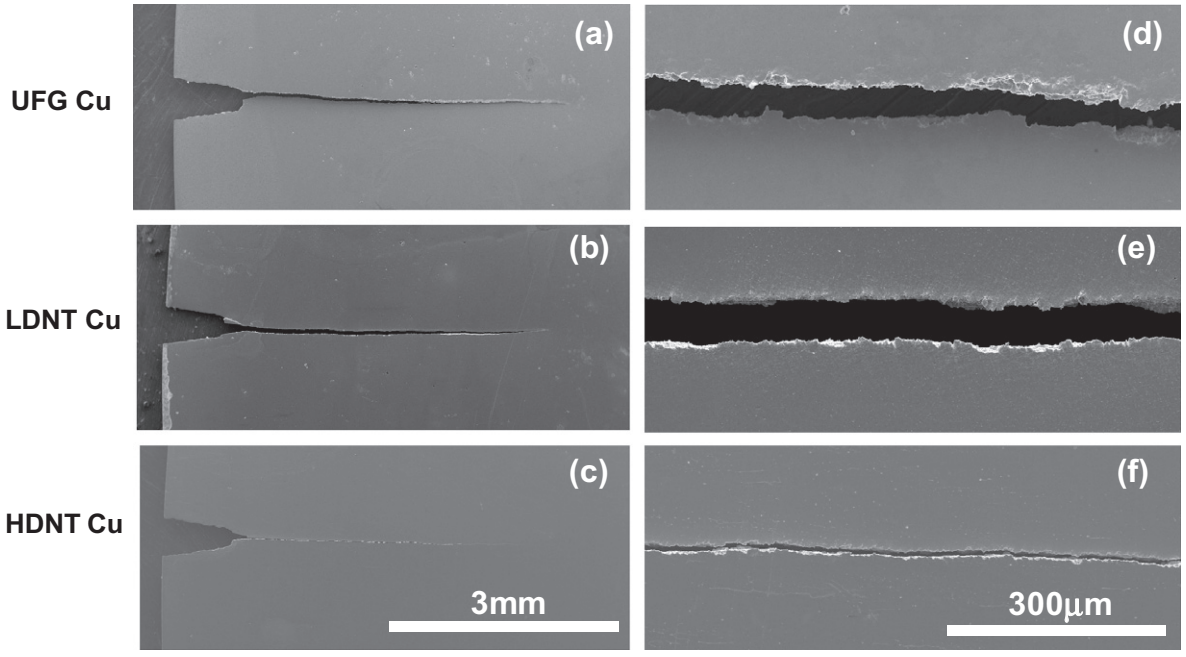

Fig. 6. SEM images of UFG (a), LDNT (b) and HDNT Cu (c) subjected to load-controlled cyclic loading at a frequency of 10 Hz. (d), (e) and (f) are higher magnification images of (a), (b) and (c) respectively. The three crack profiles are similar in terms of crack path tortuosity, deflection angle and surface roughness, showing that these parameters are not significantly influenced by the twin density (given that the grain size is essentially the same for the three cases).

tion threshold as a function of mechanical properties also support this observation. For example, models proposed by Donahue et al. [54] suggest that the threshold for the beginning of perceptible crack growth occurs when the crack tip opening displacement becomes comparable to the critical microstructural length scale.

$$\Delta K_{th} \propto \sqrt{\sigma_y E l^*} \tag{8}$$

where l^* is the relevant microstructural length scale. It has been shown by Yoder et al. [55] that cyclic plastic zone size instead of the CTOD needs to reach a critical microstructural length scale in order to reach the transition threshold, leading to the formulation

$$\Delta K_T \propto \sigma_y \sqrt{l^*} \tag{9}$$

Proceeding on the same lines, the threshold is also postulated to be attained when the shear stress needed to nucleate and move a dislocation reaches a critical value [56]:

$$\Delta K_{th} \propto \tau \sqrt{b} \tag{10}$$

where b is the magnitude of the Burgers vector. Although all these formulations do not exactly capture all the complexities of the structural variations possible, they underscore the notion that threshold decreases with a decrease in structural length scale but increases with an increase in strength. In the present study the grain size is kept constant for all the cases; however, the strength increases with an increase in twin density. These models capture our result of the fatigue transition threshold increasing with twin density, as the grain size (not the twin lamellar thickness) is the critical microstructural length scale.

For stage II fatigue crack growth, the crack advances by a process of duplex slip along two slip systems [57]. This results in a planar (mode I) crack advance normal to the loading axis. The growth in stage II is not found to be microstructure sensitive, unlike stage I. Unlike the faceted fracture surface in stage I, the fracture surface in stage II normally shows striations. The crack advance is shown to occur via crack tip blunting and the striations manifest the amount of crack extension in one cycle in most ductile fcc metals. In the current study, no obvious striations were observed in all specimens tested. However, as can be seen in Fig. 4, the rate of crack growth is lowest for HDNT Cu and increases with a decrease in twin density.

Subsequent to stage II fatigue crack growth, the crack advances rapidly and the specimens are expected to fail in a ductile manner by void nucleation and growth. It can be seen in Fig. 7 that fracture toughness of Cu is enhanced by decreasing the twin lamellar spacing. However, an opposite trend has been observed in earlier studies for nanograined materials, where grain refinement leads to poor damage tolerance and diminished values of fracture toughness [15,32]. Strain energy accommodation by plastic work is limited in nanograined materials due to curtailed dislocation activity, which is also one important reason behind the poor ductility of NG materials. In

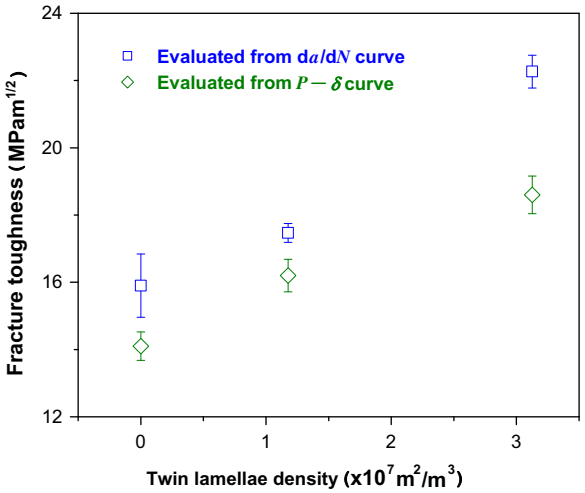

Fig. 7. Variation of fracture toughness with changes in twin density. The figure depicts the effect of twin density (or twin lamellar spacing) on the fracture toughness obtained both from the P–δ experiments and the crack propagation experiment, respectively. Increasing twin density enhances the fracture toughness of nanotwinned copper.

displacement-controlled testing, high stress concentration at the grain boundaries arises due to limited plasticity for NG metals, which makes the process of void nucleation at the grain boundaries even more severe. However, increasing twin density can lead to enhanced plastic strain accommodation due to the high area of twin boundaries, which are principal sites for accumulation and pile-up of partial dislocations. This, in turn, could contribute to enhanced values of fracture toughness, as has been observed in the current study.

5. Conclusion

This work reveals for the first time that high twin density in UFG copper provides a unique combination of strength, ductility, fracture initiation resistance and damage tolerance during stable fatigue crack growth. The fracture toughness values show marked improvement with the introduction of nanotwins. During fatigue crack growth, grain and twin refinement are different mechanistic processes in terms of their influence on crack path tortuosity and crack surface roughness. Because twin planes are also slip planes in fcc metals and there exists strong plastic anisotropy, this suggests that stage I fatigue crack propagation is likely to occur parallel to the twin planes within each grain along the crack path and thus these intra-grain twin planes, unlike grain boundaries, can more easily facilitate stage I, serrated (and locally non-mode I) fracture trajectory. Electron microscopy investigations would be helpful to further confirm these inferences. Indeed, our study has shown that HDNT Cu, which has the highest strength, also showed relatively the best fatigue crack growth resistance. On the other hand, UFG Cu with essentially no nanotwins showed the poorest plane stress fatigue initiation toughness and subcritical fatigue crack growth

response of the three materials studied here. In spite of their unique combination of properties, it is challenging at this time to produce homogeneously nanotwinned Cu in bulk, which is essential if it is to be employed in any structural applications. It is also not yet an easy task to introduce nanotwins in many other important structural materials. Further progresses in processing methods would help exploit the beneficial damage-tolerant properties identified in this work for metals containing coherent nanoscale twins.

Acknowledgments

The authors would like to acknowledge the financial support by the ONR Grant N00014-08-1-0510, as well as a research grant provided by Schlumberger Limited. S.S. and M.D. further acknowledge support from the Advanced Materials for Micro and Nano Systems Programme of the Singapore-MIT Alliance (SMA). L.L. acknowledges the financial support from the National Science Foundation of China (Grant Nos. 50725103, 50890171 and 51071153), Most International S&T Cooperation project of China (S2011ZR0270), and the Danish National Research Foundation and the National Natural Science Foundation of China (Grant No. 50911130230) for the Danish–Chinese Center for Nanometals. The authors are grateful to Mr. S. Jin for sample preparation.

References

[1] Siegel RW, Fougere GE. Nanostruct Mater 1995;6(1–4):205–16.
[2] Sanders PG, Eastman JA, Weertman JR. Acta Mater 1997;45(10):4019–25.
[3] Gleiter H. Acta Mater 2000;48(1):1–29.
[4] Wang YM, Chen MW, Zhou FH, Ma E. Nature 2002;419(6910):912–5.
[5] Kumar KS, Van Swygenhoven H, Suresh S. Acta Mater 2003;51(19):5743–74.
[6] Dao M, Lu L, Asaro RJ, De Hosson JTM, MA E. Acta Mater 2007;55(12):4041–65.
[7] Suresh S. Fatigue of materials. 2nd ed. Cambridge: Cambridge University Press; 1998.
[8] Hanlon T, Kwon YN, Suresh S. Scripta Mater 2003;49(7):675–80.
[9] Mishra R, Balasubramaniam R. Corros Sci 2004;46(12):3019–29.
[10] Hanlon T, Tabachnikova ED, Suresh S. Int J Fatigue 2005; 27(10–12):1147–58.
[11] Hanlon T, Chokshi AH, Manoharan M, Suresh S. Int J Fatigue 2005;27(10–12):1159–63.
[12] Schuh CA, Nieh TG, Yamasaki T. Scripta Mater 2002;46(10):735–40.
[13] Schwaiger R, Moser B, Dao M, Chollacoop N, Suresh S. Acta Mater 2003;51(17):5159–72.
[14] Suresh S, Li J. Nature 2008;456(7223):716–7.
[15] Mirshams RA, Mao CH, Whang SH, Yin WM. Mater Sci Eng A 2001;315(1–2):21–7.
[16] Callister WD. Materials science and engineering, an introduction. 5th ed. New York: Wiley; 2000.
[17] Brandes EA, Brook GB. Smithells metals reference book. 7th ed. Oxford: Butterworth; 1998.
[18] Andrews PV, West MB, Robeson CR. Philoso Mag 1969;19(161):887–98.
[19] Pry RH, Hennig RW. Acta Metall 1954;2(2):318–21.
[20] Freund LB, Suresh S. Thin film materials. New York: Cambridge University Press; 2003.
[21] Witney AB, Sanders PG, Weertman JR, Eastman JA. Scripta Metall Mater 1995;33(12):2025–30.
[22] Agnew SR, Weertman JR. Mater Sci Eng A-Struct 1998;244(2):145–53.
[23] Agnew SR, Vinogradov AY, Hashimoto S, Weertman JR. J Electron Mater 1999;28(9):1038–44.
[24] Mughrabi H, Höppel HW. Mater Res Soc Symp 2001;634:B2.1.1–B2.1.12.
[25] Hoppel HW, Zhou ZM, Mughrabi H, Valiev RZ. Philos Mag A 2002;82(9):1781–94.
[26] Moser B, Hanlon T, Kumar KS, Suresh S. Scripta Mater 2006;54(6):1151–5.
[27] Fan GJ, Fu LF, Wang GY, Choo H, Liaw PK, Browning ND. J Alloys Compd 2007;434:298–300.
[28] Yang Y, Imasogie B, Fan GJ, Liaw PK, Soboyejo WO. Metall Mater Trans A 2008;39A(5):1145–56.
[29] Farkas D, Van Petegem S, Derlet PM, Van Swygenhoven H. Acta Mater 2005;53(11):3115–23.
[30] Xie JJ, Wu XL, Hong YS. In: Yang W, Geni M, Wang TJ, Zhuang Z, editors. Advances in fracture and materials behavior, Pts. 1 and 2, vol. 33–37. 2008. p. 925–30.
[31] Trusov LT, Gryaznov VG. Growth of crystals. New York: Consultants Bureau; 1991. p. 55.
[32] Karimpoor AA, Erb U. Phys Status Sol A 2006;203(6):1265–70.
[33] Ovid'ko IA, Sheinerman AG. Acta Mater 2010;58(16):5286–94.
[34] Lu L, Schwaiger R, Shan ZW, Dao M, Lu K, Suresh S. Acta Mater 2005;53(7):2169–79.
[35] Dao M, Lu L, Shen YF, Suresh S. Acta Mater 2006;54(20):5421–32.
[36] Lu L, Dao M, Zhu T, Li J. Scripta Mater 2009;60(12):1062–6.
[37] Lu K, Lu L, Suresh S. Science 2009;324(5925):349–52.
[38] Lu L, Zhu T, Shen YF, Dao M, Lu K, Suresh S. Acta Mater 2009;57(17):5165–73.
[39] Christian JW, Mahajan S. Prog Mater Sci 1995;39(1–2):1–157.
[40] Shen YF, Lu L, Lu QH, Jin ZH, Lu K. Scripta Mater 2005;52(10):989–94.
[41] Lu L, Shen YF, Chen XH, Qian LH, Lu K. Science 2004;304(5669):422–6.
[42] Sutton AP, Ballufi RW. Interfaces in crystalline materials. Oxford: Oxford University Press; 1995.
[43] Shute CJ, Myers BD, Xie S, Barbee TW, Hodge AM, Weertman JR. Scripta Mater 2009;60(12):1073–7.
[44] Tang L, Lu L. Acta Metall Sin 2009;45(7):808–14.
[45] Cheng S, Zhao YH, Wang YM, Li Y, Wang XL, Liaw PK, et al. Phys Rev Lett 2010;104(25):255501.
[46] Zhou HF, Qu SX, Yang W. Model Simul Mater Sci Eng 2010;18(6):065002.
[47] Zhou HF, Qu SX. Nanotechnology 2010;21(3):035706.
[48] Qin EW, Lu L, Tao NR, Tan J, Lu K. Acta Mater 2009;57(20):6215–25.
[49] Anderson TL. Fracture mechanics: fundamentals and applications. 2nd ed. Boca Raton, FL: CRC Press; 1994.
[50] Hertzberg RW. Deformation and fracture mechanics of engineering materials. 4th ed. New York: John Wiley and Sons; 1996.
[51] ASTM E399. Standard test method for linear-elastic plane-strain fracture toughness K_{IC} of metallic materials. West Conshohocken, PA: ASTM International; 2009.
[52] Suresh S. Metall Trans A 1985;16(2):249–60.
[53] Shih CF. J Mech Phys Sol 1981;29(4):305–26.
[54] Donahue RJ, Clark HM, Atanmo P, Kumble R, McEvily AJ. Int J Fract Mech 1972;8(2):209–19.
[55] Yoder GR, Cooley LA, Crooker TW. Eng Fract Mech 1979;11(4):805.
[56] Sadananda K, Shahinian P. Int J Fract 1977;13(5):585–94.
[57] Forsyth P. Crack propagation. In: Proceedings of cranfield symposium; 1962. p. 76–94.